Environmental Science & Technology

Article

Cite This: Environ. Sci. Technol. 2019, 53, 3268−3276

pubs.acs.org/est

# Conserved Microbial Toxicity Responses for Acute and Chronic Silver Nanoparticle Treatments in Wetland Mesocosms

Christopher S. Ward,[†,‡,#] Jin-Fen Pan,[†,§,#] Benjamin P. Colman,[∥] Zhao Wang,[†] Carley A. Gwin,[⊥] Tiffany C. Williams,[†] Abby Ardis,[†] Claudia K. Gunsch,[⊥] and Dana E. Hunt*[,†,‡,∥,⊥]

[†]Marine Laboratory, Duke University, Beaufort, North Carolina 28516, United States

[‡]Program in Environmental Health and Toxicology, Duke University, Durham, North Carolina 27708, United States

[§]Key Laboratory of Marine Environment and Ecology (Ministry of Education), College of Environmental Science and Engineering, Ocean University of China, Qingdao, 266003, P. R. China

[∥]Biology Department, Duke University, Durham, North Carolina 27708, United States

[⊥]Civil and Environmental Engineering, Duke University, Durham, North Carolina 27708, United States

Supporting Information

**ABSTRACT:** Most studies of bacterial exposure to environmental contaminants focus on acute treatments; however, the impacts of single, high-dose exposures on microbial communities may not readily be extended to the more likely scenario of chronic, low-dose contaminant exposures. Here, in a year-long, wetland mesocosm experiment, we compared microbial community responses to pulse (single 450 mg dose of silver) and chronic (weekly 8.7 mg doses of silver for 1 year) silver nanoparticle ($Ag^0$ NP) treatments, as well as a chronic treatment of "aged" sulfidized silver nanoparticles ($Ag_2S$ NPs). While mesocosms exposed to $Ag_2S$ NPs never differed significantly from the controls, both $Ag^0$ NP treatments exhibited reduced microbial diversity and altered community composition; however, the effects differed in timing, duration, and magnitude. Microbial community-level impacts in the acute $Ag^0$ NP treatment were apparent only within the first weeks and then converged on the control mesocosm composition, while chronic exposure effects were observed several months after exposures began, likely due to interactive effects of nanoparticle toxicity and winter environmental conditions. Notably, there was a high level of overlap in the taxa which exhibited significant declines (>10×) in both treatments, suggesting a conserved toxicity response for both pulse and chronic exposures. Thus, this research suggests that complex, but short-term, acute toxicological studies may provide critical, cost-effective insights into identifying microbial taxa sensitive to long-term chronic exposures to Ag NPs.

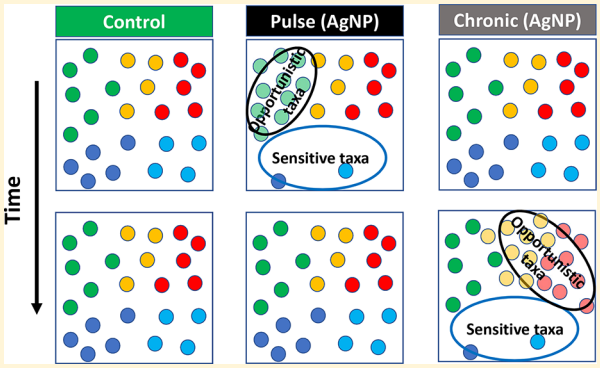


## INTRODUCTION

Silver nanoparticles (Ag NPs) are commonly used in consumer products, including textiles that resist odor-causing bacteria, plastic containers, and medical devices, largely due to their antimicrobial properties. As annual production of Ag NPs is estimated to reach 250 tons in the United States and Europe alone,[1,2] these nanoparticles will inevitably make their way into residential and industrial waste streams,[2,3] with significant environmental releases through wastewater treatment plant effluent or land-applied biosolids.[2,4] Previous investigations of Ag NPs have observed toxicity across a wide range of organisms, including reduced growth and germination rates in plants,[5,6] inhibition of photosynthesis in algae,[7−9] and increases in shellfish oxidative stress biomarkers.[10] Studies specifically focusing on microorganisms and microbial processes have found that Ag NP treatments alter community composition, lower community diversity, and reduce rates of key biogeochemical processes.[11−15] As Ag NPs' antimicrobial properties are likely due to a combination of cell membrane disruption, reactions with cellular components such as DNA, and oxidative stress,[16,17] they have been shown to be toxic in a broad phylogenetic range of microbes; however, all bacterial taxa are not equivalently sensitive to Ag NP toxicity.[14,18,19] Moreover, our ability to predict Ag NP impacts on the environment is limited, as many microbial toxicity studies have been conducted with pure cultures[7,16] or low-complexity communities under controlled laboratory conditions,[11,13] and thus may not capture the diversity of microbial types and the range of conditions present in complex, natural environments.[20,21]

Received: November 25, 2018
Revised: February 11, 2019
Accepted: February 18, 2019
Published: February 18, 2019






DOI: 10.1021/acs.est.8b06654
Environ. Sci. Technol. 2019, 53, 3268−3276

Recent nanomaterial mesocosm experiments have increased the environmental complexity of the systems examined, but the short experimental duration[22] or limited replication in light of high biological variability among replicate mesocosms[23] can prevent extrapolation to realistic environmental exposure scenarios that include bioaccumulation and trophic transfer.[21] Additionally, many studies examine only freshly synthesized nanoparticles when nanoparticle mobility and toxicity are altered by interactions with organic material, organisms, and anaerobic conditions.[10,24,25] Moreover, microbial Ag NP studies do not always agree on the specific taxa that increase or decrease due to Ag NP treatment,[11,13,26] making it difficult to draw general conclusions about the potential impacts of Ag NPs on environmental microbiomes. Thus, despite the extensive literature examining the environmental impacts of silver nanomaterials, the predicted impact of these particles on microbial communities in natural environments, specifically a comparison of acute and chronic exposures, remains to be determined.

Here, we use a replicated wetland mesocosm design to compare changes in water column microbial community composition in response to pulse and chronic silver nanoparticle exposures. This study contrasts "spill" conditions, e.g., $Ag^0$ NP applied as a single pulse dose of 450 mg of silver, with environmentally realistic chronic loading[27] (8.7 mg of silver weekly for 1 year, total amount = 450 mg) of either pristine ($Ag^0$ NP) or "aged" sulfidized silver nanoparticles ($Ag_2S$ NPs). In anaerobic environments, Ag NPs are converted to less toxic $Ag_2S$ NPs, which may represent a more realistic environmental exposure route.[4,25,28] These mesocosms were followed over the course of a year allowing for long-term exposure, variability in a range of environmental parameters, as well as movement of the nanoparticles through the ecosystem, and the microbial communities in these treatments were compared by 16S rRNA gene library sequencing. In the pulse mesocosms, we anticipated a rapid microbial community change that would gradually return to resemble the control communities (resilience),[29] while the chronic treatment microbial communities would more slowly diverge from the controls, likely with reduced impacts on the microbial community composition in chronic mesocosms treated with $Ag_2S$ NPs compared to those dosed with $Ag^0$ NPs.

## MATERIALS AND METHODS

**Mesocosms.** This study took place at the Center of Environmental Implications of Nanotechnology (CEINT) mesocosm facility in the Duke University Forest (Durham, North Carolina, USA) from August 2013 to August 2014. The overall design and construction of wetland mesocosms was described previously:[28,30−32] a slant board mesocosm, consisting of a permanently flooded aquatic zone (~610 L), a transition zone, and an upland zone. The mesocosms were filled on the same day with well water from the site. To simulate dispersal and connectivity with a larger wetland system, mesocosms were inoculated every 2 weeks with 250 mL of 200 $\mu$m filtered water from a local wetland, in periods it was not frozen. To prevent mesocosms from freezing or overflowing with spring rains, a heated greenhouse covered the mesocosms from December 11, 2013, to April 29, 2014. Organisms were added to or allowed to colonize the mesocosms including *Egeria densa* (waterweed), *Physella acuta* (pond snails), larval *Libellulidae* (dragonflies), *Gambusia holbrookii* (Eastern mosquitofish), *Corbicula fluminea* (Asiatic clam), and *Landoltia punctata* (duckweed) starting 180 days before the onset of mesocosm dosing.

**Silver Nanoparticles (Ag NPs).** Gum arabic-coated silver nanoparticles were freshly synthesized by CEINT, with a mean transmission electron microscopy-measured diameter of 3.9 ± 1.7 nm (mean ± SD, $n$ = 159).[33] These $Ag^0$ NPs were then sulfidized through exposure to thioacetamide,[34] yielding spherical particles of mean diameter 24.2 ± 6.0 nm (mean ± SD, $n$ = 155) with an X-ray powder diffraction (XRD) pattern consistent with acanthite.[30] Particles were purified and concentrated by diafiltration, and suspensions were periodically checked to confirm that no changes in particle size or concentration had occurred during storage.

**Experimental Treatments.** A total of 12 mesocosms were subjected to one of four treatments (three replicate mesocosms per treatment): control without nanoparticles (Ctrl), pulse zerovalent silver NPs (P-$Ag^0$ NPs), chronic zerovalent silver NPs (C-$Ag^0$ NPs), and chronic sulfidized silver NPs (C-$Ag_2S$ NPs) treatments from stock solutions of 1.96 g Ag $L^{-1}$ (Figure S1). Prior to dosing, treatments were assigned so that variation in environmental parameters (e.g., chlorophyll *a*) was distributed across treatments. For the pulse $Ag^0$ NPs treatment, 450 mg of silver as gum arabic-coated Ag NPs suspended in mesocosm water was added on day 0 (August 13, 2013) evenly across the aquatic portion of the mesocosm, resulting in an expected initial concentration of 0.74 mg Ag $L^{-1}$. This treatment is intended to simulate a spill or sudden release of large quantities of Ag NPs immediately upstream of a wetland environment, similar to previous "pulse" studies.[31] In contrast, chronic treatments represent gradual additions of a pollutant as might occur downstream of a wastewater treatment plant[27] and consisted of weekly additions of 8.7 mg of silver as gum arabic-coated $Ag^0$ NPs or $Ag_2S$ NPs were added to the mesocosm water weekly for 1 year. Thus, despite differences in dosing regime, over the course of the study, all NP treatments received 450 mg of Ag NPs applied to the aquatic portion of the mesocosm.

**Sample Collection.** Environmental metadata including temperature and dissolved oxygen were collected as previously described.[31] To measure total Ag, subsamples of whole water were collected and acidified to 0.15 M $HNO_3$ to dissolve Ag, which was quantified by inductively coupled plasma mass spectrometry using an Agilent 7500cx.[32] Silver concentration data are presented as the time-weighted average, which is an approximation of the average concentrations organisms are exposed to over the course of each weekly addition.[32] Briefly, the method entails the averaging of the sum of the products of the log transformed concentration data and the duration of time between sampling points, which is then divided by the 7 days between each addition. To examine the microbial community, the aquatic zone was sampled at least quarterly from August 2013 to August 2014, with higher frequency sampling during the first month (days 0, 1, 3, 7, 14, and 28), in order to capture the anticipated rapid, transient responses to nanomaterial additions. From each mesocosm, 300 mL of water was collected from near-surface (~0.25 m depth) by submerging sterile polypropylene bottles. Samples for flow cytometry were fixed in the lab with net 0.5% glutaraldehyde and stored at −80 °C until analysis. Microbial biomass was collected from 250 mL of water on 0.22 $\mu$m Supor filters (Pall) via gentle vacuum filtration upon return to the lab. Samples were stored at −80 °C until DNA extraction.



DOI: 10.1021/acs.est.8b06654
Environ. Sci. Technol. 2019, 53, 3268−3276

Table 1. Mean Weekly Water Temperature (°C) across All Treatments and Time Weighted Average Silver Concentration ($\mu$g $L^{-1}$) in the Mesocosm Water Column

| | | | time weighted average Ag concentration[a] ($\mu$g $L^{-1}$) | | |
|---|---|---|---|---|---|
| week | microbiome sample day(s) | water temperature[b] (°C) | pulse $Ag^0$ NP | chronic $Ag^0$ NP | chronic $Ag_2S$ NP |
| 1 | 1, 3, 7 | 23.3 ± 0.7 | 463 ± 130 | 7.26 ± 2 | 13.9 ± 3.8 |
| 2 | 10, 14 | 25.8 ± 0.6 | 125 ± 34 | 9.25 ± 2.9 | 16.1 ± 4.3 |
| 4 | 28 | 25.6 ± 0.4 | 7.47 ± 2.0 | 8.09 ± 2.2 | 12 ± 3.2 |
| 14 | 98 | 9.33 ± 1.4 | 0.159 ± 0.043 | 1.95 ± 0.53 | 13.5 ± 3.7 |
| 18 | 126 | 6.76 ± 0.5 | 0.25 ± 0.068 | 9.01 ± 2.4 | 11.6 ± 3.1 |
| 29 | 203 | 13.7 ± 0.4 | 0.0804 ± 0.022 | 13.5 ± 3.6 | 9.82 ± 2.7 |
| 39 | 273 | 23.1 ± 0.4 | 0.248 ± 0.067 | 16.2 ± 4.4 | 18.4 ± 5.0 |
| 47 | 333 | 26.4 ± 0.6 | 0.306 ± 0.083 | 6.85 ± 1.9 | 10.2 ± 2.8 |
| 52 | 364 | 25.7 ± 0.7 | 0.0832 ± 0.022 | 2.91 ± 0.79 | 4.13 ± 1.1 |

[a]Silver in control mesocosms averaged 0.008 ± 0.001 $\mu$g $L^{-1}$. [b]Data is presented as the average ± standard error of the mean (temperature, $n$ = 7; time weighted average Ag, $n$ = 3).

**DNA Extraction and Sequencing.** DNA extraction was performed according to the manufacturer's instructions (Gentra Puregene kit; QIAGEN), with the addition of bead beating for 3 × 30 s at 4800 rpm. The DNA concentration was quantified with a nanodrop (Thermo Fisher). The V3−V4 region of the 16S rRNA gene was amplified and bar-coded using primers targeting the bacterial and archaeal 16S rRNA genes: 16S F V3, CCTACGGGNGGCWSCA, and 16S R V4, GGACTACNVGGGTWTCTAAT.[35,36] PCR amplification was carried out in a total volume of 20 $\mu$L containing 20 ng of template DNA, 200 $\mu$M dNTPs, 2 mM $MgCl_2$, 0.5 $\mu$M primers, and 0.4 U of Q5 DNA polymerase (NEB). The PCR thermocycling conditions were 98 °C for 30 s and 28 cycles at 98 °C for 10 s, 55 °C for 30 s, and 72 °C for 30 s, with a final extension at 72 °C for 2 min. Triplicate reactions per sample were pooled and gel purified. In total, 119 libraries were sequenced on the Illumina MiSeq using the 2× 250 nt paired-end protocol at Duke's Genome Sequencing and Analysis Core Facility. Sequences were deposited to NCBI's Sequence Read Archive as Bioproject SRP132123.

**Sequence Processing.** Sequences were demultiplexed and assigned to corresponding samples using CASAVA (Illumina). Sequences were then processed in USEARCH v7.[37,38] Briefly, sequence reads were trimmed using a 10-nt running window with a minimum mean Phred quality (Q) score of 30. Paired-end reads were merged (≥10 nt overlap without mismatches), and the resulting contigs were quality-filtered to remove reads with expected errors >0.5 or shorter than 400 nt. Sequence contigs were then dereplicated, and singletons were discarded. Contigs were clustered into operational taxonomic units (OTUs) of at least 97% similarity using the centroid-based clustering UPARSE-OTU algorithm[38] with a pairwise identity of 98.5% to the centroid. The OTU clustering step includes the removal of reads containing chimeric models, and an additional reference-based chimera filtering step was performed using UCHIME[39] with the ChimeraSlayer reference database version microbiomeutil-r20110519, resulting in 2,523,559 total sequences and 11,638 OTUs after processing. Libraries contained between 9574 and 33,207 sequences; to control for uneven sequencing effort, we normalized the data by rarefaction to 9574 sequences per sample. Taxonomy was assigned to the most abundant sequence in each OTU using the Greengenes database (release 13_8), and the rRNA operon copy number was corrected with CopyRighter.[40]

**Flow Cytometry and Library Relative Abundance Normalization.** Microbial abundances were enumerated using a BD FACSCalibur Flow Cytometer. Samples for quantification of phytoplankton used natural pigments, while in quantification of total prokaryotes samples were first stained with SYBR Green-I.[41] One of the criticisms of 16S rRNA gene libraries to examine changes in microbial communities is that library relative abundance does not accurately reflect the abundance of members of the microbial community. Here, we attempt to correct for the impact abundance changes in one population can have on the relative abundance of other taxa in the same library by calculating an "absolute abundance" metric for each OTU by multiplying the [total prokaryotic cells $mL^{-1}$] by the [relative abundance in an rRNA operon number corrected 16S rRNA gene library] to yield an "absolute abundance" in cells $mL^{-1}$. While these numbers should not be interpreted as true cell counts due to a number of biases and limitations involved in both flow cytometry-based bacterial enumeration and amplicon sequencing,[42−44] they provide additional context to changes in library relative abundances, particularly when total cell abundances differ. In this study, a decrease in absolute abundance strengthens our interpretation of toxicity or direct negative responses to Ag NP treatment.

**Statistical Analyses.** Statistical analyses were performed using the *vegan* package in R, unless otherwise noted. The OTU absolute abundance table was log-transformed to reduce the distortion due to sparse matrixes. In comparisons of community composition, the homogeneity of data variance was confirmed using the *betadisper* function. Community compositional differences by treatment were compared using permutational multivariate analysis of variance (PERMANOVA, *adonis*) on a Bray−Curtis distance matrix with 999 random permutations, and when the results were significant ($p < 0.05$), the post hoc Tukey HSD test was applied. Community variance was visualized using weighted Bray−Curtis dissimilarity via nonmetric multidimensional scaling (NMDS). Identification of indicator taxa for each of the treatments was performed using the linear discriminant analysis effect size (LEfSe).[45] In visualizing this data, we normalized the average absolute abundance within a treatment to the controls to account for seasonal changes in the abundance of specific OTUs (Figure S4). We statistically identified OTUs that were differentially abundant compared to controls in the NP treatments using DESeq2:[46] absolute abundances for 97% identity OTUs were adjusted with an added pseudo count of 1 to avoid excessive zeros inflating the model. Significant differences were identified for comparisons with a minimum |fold change| ≥ 2, relative to the control mesocosms and a $p$



DOI: 10.1021/acs.est.8b06654
Environ. Sci. Technol. 2019, 53, 3268−3276

value <0.05 (adjusted for multiple hypothesis testing using the Benjamini−Hochberg method). Time-weighted average silver concentration data were compared and standard errors generated using the lme4 and lsmeans packages, as described previously.[32] Time-weighted average concentration data were fit to a generalized linear mixed effects model using the glmer function with a gamma distribution for the family and a log link with treatment nested within time and mesocosm as a random effect.

## RESULTS AND DISCUSSION

**Pulse $Ag^0$ NP (P-$Ag^0$ NP) Treatment.** In this study, we specifically contrast introduction of $Ag^0$ nanoparticles as a single large pulse with weekly chronic additions of $Ag^0$ NPs and "aged" $Ag_2S$ NPs into replicated freshwater wetland mesocosms (Figure S1). As microbial communities respond to seasonal and episodic changes,[42] we focus on comparing Ag NP treatments to control mesocosms at each time point rather than changes within a given mesocosm type over time. In this experiment, the pulse Ag NP treatment caused rapid changes in the mesocosm conditions, with high aquatic silver concentrations (Table 1), reductions in dissolved oxygen (Table S1, two-way ANOVA, days 1 and 2, $p < 0.05$), and decreases in total prokaryotic cell concentrations (Figure 1A; two-way ANOVA, days 3 and 7, $p < 0.05$). These results point to a toxic response with the death of sensitive bacterioplankton, concurrent with observed membrane damage in aquatic plants.[30] Both plant damage and microbial cell death likely released organic matter which was degraded by the microbial community, drawing down levels of oxygen (Table S1). Overall, these results agree with those of a previous experiment examining ecosystem responses to pulse doses of Ag NPs in wetland mesocosms.[31] However, phytoplankton concentrations (Figure 1B) did not decline following nanoparticle dosing, as was observed in a previous experiment with an initial silver concentration >3× higher of 2.5 mg $L^{-1}$ as Ag NPs,[31] which may be due to the higher nanoparticle dose in the previous experiment or differentially sensitive phytoplankton communities.

Additionally, microbial community characteristics and composition offer further insights into the toxicity of Ag NPs. The pulse treatment microbial community exhibited a rapid and dramatic response to Ag NP dosing, with a statistically significant decrease in Shannon's diversity (Figure 2, on days 1, 3, and 7), which apparently persisted (although not at a statistically significant level) until day 28. This result is consistent with the reduced diversity and evenness of microbial communities reported previously following Ag NP treatment.[29,47] However, the most dramatic response to $Ag^0$ NP addition was in microbial community composition; P-$Ag^0$ NP mesocosm microbial communities statistically differed from both the controls and the other NP treatments (Figure 3) and separated from all other treatments in nonmetric multidimensional scaling (NMDS) ordination (Figure S2) on days 1−7. These microbial community differences between controls and the pulse $Ag^0$ NP treatment were due to library dominance by a single *Flectobacillus* operational taxonomic unit (OTU; phylum *Bacteroidetes*, Figures S3 and S4), in agreement with a previous study showing *Bacteroidetes* increased following Ag NP additions.[13] Despite an overall decline in bacterioplankton cell abundances at early time points in the P-Ag NP treatment mesocosms (Figure 1A), the absolute abundance of this single OTU in the pulse treatment was roughly 100× higher than

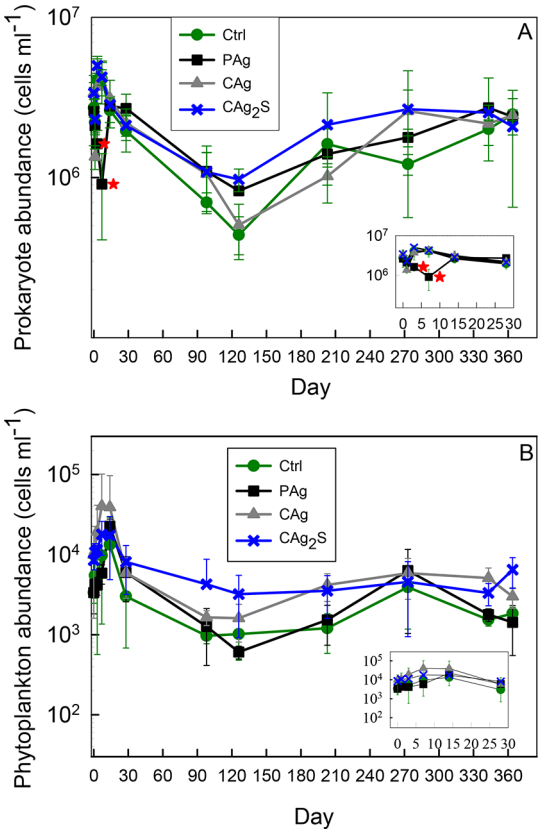


**Figure 1.** Prokaryote and phytoplankton cell abundances in pulse and chronic silver nanoparticle-dosed mesocosms. (A) Prokaryotic and (B) phytoplankton cell counts in the aquatic portion of the mesocosms over time. Numbers presented are mean ± one standard deviation ($n = 3$); lower error bars are not shown when one mean-standard deviation <0. Ctrl, control (green); P-Ag, pulse $Ag^0$ NP (black); C-Ag, chronic $Ag^0$ NP (gray); C-$Ag_2S$, chronic $Ag_2S$ NP (blue). Statistical comparisons using two-way ANOVA comparisons between control and nanoparticle-treated mesocosms ($n = 3$); a red asterisk indicates a statistically significant decrease for P-Ag prokaryotic cell concentrations of days 3 and 7 ($p < 0.05$) relative to the control. The day is relative to the onset of nanoparticle dosing on day 0; the inset is used to show time points in the first month at higher resolution.

that in the control mesocosms (Figure S4; Tukey HSD, $p < 0.05$). Pulse disturbances frequently enrich the microbial community with resistant and/or opportunistic populations,[29,47] which are tolerant of the disturbance conditions, and can capitalize on resource availability or reduced competition,[48] suggesting that this strain could be silver resistant and/or make use of the disturbed conditions, for example, organic matter release by dying organisms.

Although the dominant signal in the microbial communities at these early time points was the dramatic increase of *Flectobacillus*, it is important not to overlook the potential indications of a toxic response (Figure 3). The pulse treatment exhibited declines relative to the controls in taxa spread throughout the phylogenetic tree (e.g., *Actinobacteria*, *Proteobacteria*, *Verrucomicrobia*, and unicellular algae belonging to the *Cryptophyta*), supporting previous conclusions that Ag NPs are broadly toxic to microbes.[13] By day 28, the initial microbial community pulse response dissipated with no statistical difference between nanoparticle treatments (pulse $Ag^0$, chronic $Ag^0$, and chronic $Ag_2S$) and the control mesocosm


DOI: 10.1021/acs.est.8b06654
Environ. Sci. Technol. 2019, 53, 3268−3276

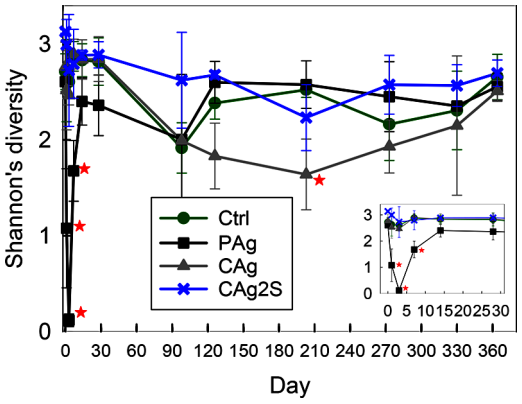


**Figure 2.** Shannon's diversity of microbial communities based on 97% identity 16S rRNA gene OTUs from the aquatic zone of nanoparticle mesocosms. Ctrl, control (green); P-Ag, pulse $Ag^0$ NP (black); C-Ag, chronic $Ag^0$ NP (gray); C-$Ag_2S$, chronic $Ag_2S$ NP (blue). Statistical comparisons using two-way ANOVA comparisons between control and nanoparticle-treated mesocosms ($n$ = 3) on specific days (a red asterisk indicates $p < 0.05$). The day is relative to the onset of nanoparticle dosing on day 0; the inset is used to show data from the first month at higher resolution.

communities (Figure 3). In summary, the pulse exposure, which is commonly used in ecotoxicological studies, had a dramatic but transient impact on the aquatic microbial community. However, following this initial disturbed period, the microbial community exhibited compositional resilience within the first month, likely due a combination of factors including removal of silver from the water column to below the acute toxicity threshold through partitioning to the soil/sediment or organisms (Table 1);[28] transformation of silver to less toxic forms (e.g., adsorption or complexation with organic material, sulfur compounds, carbonate or halogens, reducing toxicity[49,50]); and the spread of silver resistance genes through the community. While water column silver declined in the pulse treatment, weekly dosing of Ag NPs ensured that aquatic silver levels in the chronic $Ag^0$ and $Ag_2S$ treatments remained fairly constant throughout the experiment with the potential for toxicity to bioaccumulate especially at higher trophic levels over time.

**Chronic $Ag^0$ and $Ag_2S$ NP Treatments.** Silver NP dosing in the chronic $Ag^0$ (C-$Ag^0$ NP) and chronic $Ag_2S$ (C-$Ag_2S$ NP) mesocosms did not produce the same rapid, dramatic response to Ag NP exposure observed in the pulse treatment. Neither chronic treatment exhibited significant differences compared to the controls in dissolved oxygen levels or microbial cell abundances (Figure 1, Table S1). However, these environmental variables and total cell abundances are likely not as sensitive as community composition in detecting responses to anthropogenic pollutants.[51] Although we measured microbial community parameters less frequently after the first month, for all three samples from days 98−203, we observed that the chronic $Ag^0$ NP treatment altered both microbial community composition and diversity compared to control mesocosms. Mirroring the responses observed early in the pulse treatment, the microbial community exhibited decreased diversity (day 203 only) and community composition was distinct from the controls in both the PERMANOVA analyses (Figure 3) and

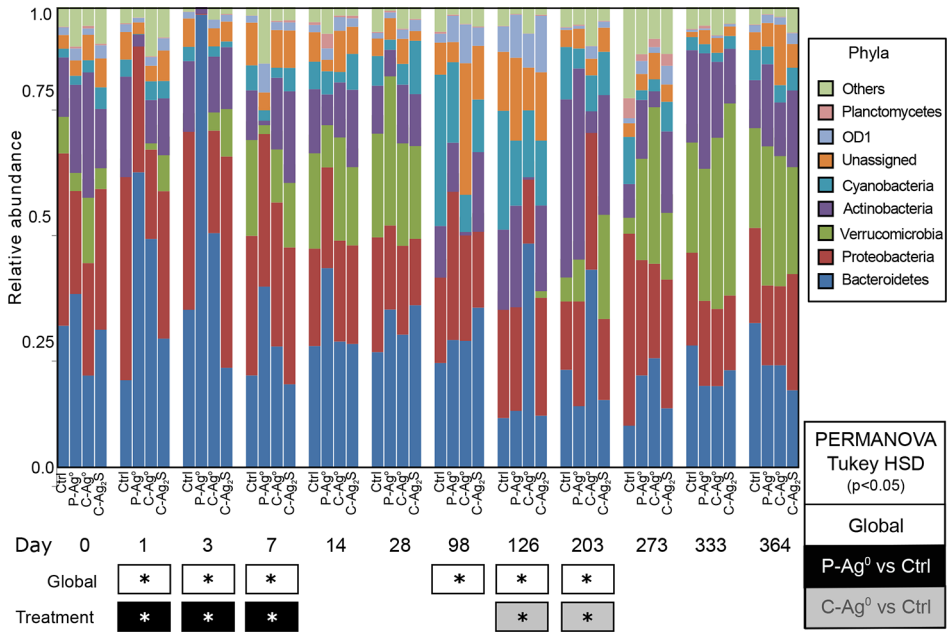


**Figure 3.** Aquatic bacterial community composition in Ag NP mesocosms based on 16S rRNA gene libraries. Average relative abundance of taxa at the phylum level for each treatment ($n$ = 3 replicates per treatment), with phyla representing <1.0% of the libraries categorized as "Others". For each day, the treatments represented are as following: Ctrl, control; P-$Ag^0$, pulse $Ag^0$ NP; C-$Ag^0$, chronic $Ag^0$ NP; C-$Ag_2S$, chronic $Ag_2S$ NP. Below the bar graph, the communities in the treatments (pulse $Ag^0$ NP, chronic $Ag^0$-NP, and chronic $Ag_2S$) are compared to the control mesocosm communities using a global PERMANOVA based on Bray−Curtis, with a white box containing an asterisk underneath that day indicating statistically significant ($p < 0.05$) differences between treatments. On days when there is a global treatment effect, Tukey's post hoc test was applied to evaluate each NP treatment against the control, with the box containing an asterisk underneath the day next to the treatment term indicating a statistically significant difference from the controls ($p < 0.05$). A black box containing an asterisk indicates a statistically significant difference between controls and the pulse $Ag^0$ NP treatment, while a gray box containing an asterisk indicates a statistically significant difference between the controls and the chronic $Ag^0$ NP treatment.



DOI: 10.1021/acs.est.8b06654
Environ. Sci. Technol. 2019, 53, 3268−3276

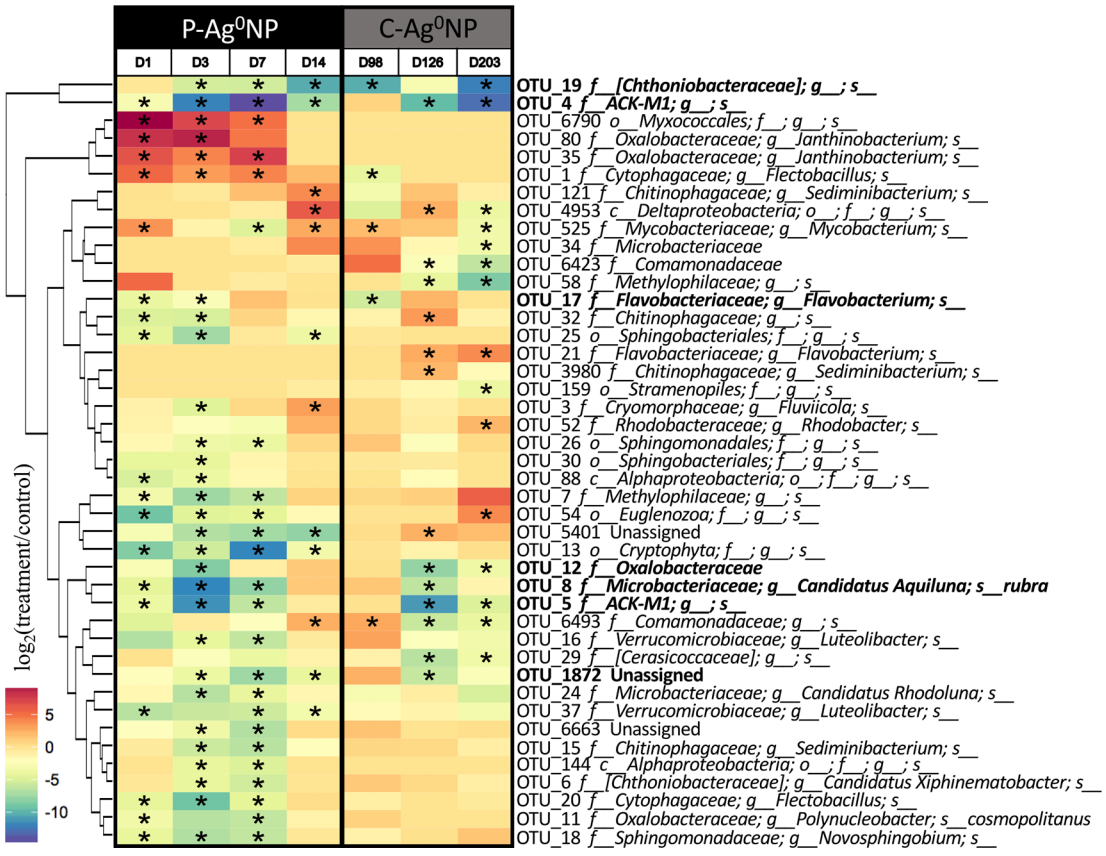


**Figure 4.** Heatmap showing sensitive microbial taxa identified in pulse and chronic $Ag^0$ NP treatments. 97% rRNA gene OTUs that changed in response to treatments were identified from periods when the community differed from the control (e.g., days 1−14 and 98−203 in the pulse and chronic $Ag^0$ NP treatments, respectively) using DESeq2. The plot includes indicator taxa (marked with asterisks) that met the following criteria: within the 20 most abundant taxa at that time point and DESeq2 identified a significant difference from the control for that OTU with a multiple-hypothesis testing corrected $p < 0.05$ and a minimum |fold change| $\geq 2$, relative to the control mesocosms. OTUs are organized by hierarchical clustering on the basis of their distribution patterns and plotted as $\log_2$(treatment/control), $n = 3$ per treatment. Greengenes-based taxonomic classification of OTUs is truncated to the family level (or the finest level if family is not unassigned: o - order, f - family, g - genus, and s - species). Potential bioindicators showing consistent statistically significant trends in both the chronic and pulse treatments are indicated by bold OTU and taxonomic identification.

NMDS plots (Figure S2). However, C-$Ag^0$ NP mesocosm microbial communities again converged on the control community composition by day 273 (Figure 3; Figure S2), despite continued high aquatic silver levels (Table 1).[32] Additionally, we never observed a microbial community-level impact of $Ag_2S$ NP additions, supporting the concept that the sulfidization process, which occurs in anaerobic, organic-rich environments such as wastewater treatment plants and wetlands,[25] likely significantly reduces the microbial toxicity of Ag NPs. Thus, chronic $Ag^0$ NP dosing exhibited later and apparently longer-lasting changes in microbial community composition compared to the pulse treatment.[29]

However, we questioned the mechanism(s) underlying the timing of the C-$Ag^0$ NP mesocosm community response (days 98−203), as these dates did not correspond to a peak in total aquatic silver concentrations (Table 1) and the effect did not persist throughout the remainder of the experiment (days 273−364). While microbial Ag NP toxicity is often attributed to the production of silver ions, a previous experiment in similar mesocosms observed rapid loss of dissolved aqueous silver (which includes $Ag^+$).[31] Moreover, there is not a simple explanation of why $Ag^+$ would be expected to increase on days 98−203, as Ag NP dissolution rates would be predicted to decrease during the low wintertime water temperatures (6−14 °C) at these time points.[52] Thus, we considered whether chronic silver toxicity impacts may have been due to interactive effects of multiple factors; multistressor research in toxicology generally focuses on co-occurring pollutants but could also include environmental factors. Due to the timing of effects and corresponding environmental conditions (winter, water temperature 6−14 °C, days 98−203; Table 1), and we calculated a statistically significant interactive effect between treatment and temperature (PERMANOVA, treatment:temperature $p = 0.036$). Explanations for the observed winter community changes in the C-$Ag^0$ NP treatments included low temperature acting as a direct stressor on microbes due to the thermodynamics of enzymes[53] or differences between organisms' optimal temperature and environmental conditions; an indirect effect on microbes mediated specific groups, e.g., primary producers; or reduced sulfidization rates (detoxification) at low temperatures. Alternatively, the microbial community may respond slowly to Ag NP loading, but resilience at later time points could be due to horizontal transfer of silver resistance genes.[54] To differentiate between these possible drivers, we examined similarities and differences in microbial community composition between the pulse and chronic contaminant exposures.


DOI: 10.1021/acs.est.8b06654
Environ. Sci. Technol. 2019, 53, 3268−3276

**Comparisons across Dosing Scenarios for Sensitive Taxa.** If similar taxa exhibit a toxicity response (e.g., decline in absolute abundance) for both pulse and chronic $Ag^0$ NP treatments, this would suggest the sensitivity of common taxa in both exposure types is due to long-term exposure toxicity or the combination of multiple stressors (likely temperature and $Ag^0$ NPs) altering the community composition directly. In order to identify $Ag^0$ NP responsive taxa, we examined the dendrogram of microbial indicator taxa (Figure S5) which groups the initial pulse $Ag^0$ NP samples (days 1−14) and the intermediate period chronic $Ag^0$ NP samples (days 98, 126, and 203), which is consistent with the timing of the NP responses in Figures 3 and S2. These data suggest that, in spite of seasonal community changes and dosing differences, there are similarities early in the pulse treatment and at intermediate time points in the chronic $Ag^0$ NP mesocosms, suggesting a conserved response to pulse and chronic Ag NP exposures. Then, to identify the specific taxa which respond to Ag NP additions, we used DESeq2 to compare initial pulse $Ag^0$ NP samples (days 1−14) and the intermediate period chronic $Ag^0$ NP samples (days 98, 126, and 203) to the control mesocosms at the same time point (Figure 4). While Figure 4 shows widespread declines in the early pulse treatment samples, the most interesting conclusion is that the seven OTUs with the largest decreases in abundance (>10×) decline in both pulse and chronic treatments (Figure 4, bold names), likely indicating a common toxic response to pollutant exposure, while taxa which increase relative to controls are not shared between exposure types. In reference to the timing of the microbial community response in the chronic treatment, bacterial temperature optima are generally higher than environmental conditions,[55] suggesting that low temperature may act as a stressor; alternately temperature may serve as a proxy for "seasonal" factors influencing microbes, such as the availability of photosynthetically fixed organic matter. Thus, additional experiments will allow determination of how seasonal effects influence microbial ecotoxicology at the community level.

In addition to increasing our insights into potential multistressor toxicity responses, Figure 4 offers a taxonomically refined view of microbial community changes following nanomaterial additions: in addition to *Flectobacillus* (OTU 1), the pulse treatment exhibits early increases in an OTU belonging to the order *Myxococcales* (phylum *Deltaproteobacteria*, OTU 6790) and two members of the family *Oxalobacteraceae* (*Betaproteobacteria*; OTUs 80 and 35) on days 1−7. In contrast, there was not a single OTU that increased across all time points shown in the chronic treatments or in both pulse and chronic treatments' sensitive periods (Figure 4). This data suggests that opportunistic taxa which increase under disturbed environmental conditions may not be good environmental contaminant indicators, as they are likely capitalizing on the disturbed conditions but may also be silver tolerant or resistant. In contrast, the toxic response is shared for both treatment types, with large (>10×) decreases in seven OTUs including members of the families *ACK-M1* (phylum *Actinobacteria*; OTUs 4 and 5), two members of the family *Microbacteriaceae* (phylum *Actinobacteria*, OTUs 8 and 1872), *Chthoniobacteraceae* (Phylum *Verrucomicrobium*; OTU 19), *Flavobacteriaceae* (phylum *Bacterioidetes*; OTU 17), and *Oxalobacteraceae* (phylum *Betaproteobacteria*; OTU 12). Interestingly, taxa with the largest decreases (>10×) were those that declined in both the pulse and chronic treatments (dark blue; Figure 4). In spite of these overall similarities, we do observe specific OTUs, for example, chloroplast sequences from the *Cryptophyta* (OTU 13) and OTU 5401 (BLAST: family *Comamonadaceae* phylum *Betaproteobacteria*) that declined significantly only in the initial P-$Ag^0$ NP treatment (Figure 4), potentially due to the very high silver concentration immediately following dosing. Moreover, aside from the sharp declines in *Actinobacteria*, likely $Ag^0$ NP-sensitive taxa are spread across common aquatic bacterial phyla, suggesting toxicity responses occur at the OTU level, not at higher taxonomic levels. As Ag NP exposure studies have been conducted in a number of environments colonized by distinct microbial communities, failure to account for OTU-level differences in Ag NP sensitivity may explain "inconsistent" reports of microbial toxicity.[11,13−15,19] Overall, although acute toxicity studies have been criticized due to their lack of environmental realism,[20] declines in similar microbial taxa across the pulse and chronic exposures suggest that we may be able to identify bacterial Ag NP bioindicators with shorter-term pulse experiments. However, it remains to be determined whether this finding can be extended to other contaminants, especially those which can be metabolized.

This experiment provides us with a unique opportunity to compare microbial community changes to pulse and chronic Ag NP pollutant exposures and may more broadly offer insights into microbial responses to environmental disturbances.[29,56] While microbial community disturbance responses have been studied extensively, as reviewed in Shade et. al,[29] few well-replicated experiments have addressed both pulse and chronic (or press in the ecology literature) treatments simultaneously, allowing comparison across exposure types. Our experiments revealed that, during the $Ag^0$ NP sensitive periods (days 1−14 in the pulse and days 98−203 in the chronic treatments), Shannon's diversity decreased (Figure 2) and the $Ag^0$ NP mesocosm microbial communities diverged from controls (Figure 3). Moreover, in spite of seasonal changes in community composition, we observed similar $Ag^0$ NP sensitive taxa in the initial time points of pulse (days 1−14) and in winter samples of the chronic mesocosms (days 98−203). Although we value the insights obtained from long-term, ecotoxicological studies to identify environmental hazards from emerging pollutants, specifically for organisms where trophic transfer and bioaccumulation are important,[32] practically, long-term experiments are not possible for all new chemicals. Thus, at least for aquatic microbes where bioaccumulation is low and community turnover is high, short-term pulse experiments may be able to identify contaminant-sensitive microbial populations and biogeochemical processes. However, future experiments are required to determine whether these results for Ag NPs can be extended to other contaminant types and environments.

## ■ ASSOCIATED CONTENT

### Supporting Information

The Supporting Information is available free of charge on the ACS Publications website at DOI: 10.1021/acs.est.8b06654.

A table of dissolved oxygen concentrations, a graphic showing the experimental design, ordination plots for the bacterial community at each time point, barplots of microbial community composition over time, *Flectobacillus* abundance in different treatments, and a heatmap



DOI: 10.1021/acs.est.8b06654
*Environ. Sci. Technol.* 2019, 53, 3268−3276

comparison of taxa that differ between treatments (PDF)

An OTU table showing the relative abundance (percentage) for the 100 most abundant OTUs (PDF)

## AUTHOR INFORMATION


### Corresponding Author

*Address: 135 Duke Marine Lab Rd, Beaufort, NC 28516; phone: (252) 504 7542; e-mail: dana.hunt@duke.edu.

### ORCID

Dana E. Hunt: 0000-0002-8801-9624


### Author Contributions

#C.S.W., J.-F.P.: Equal authorship.

### Notes

The authors declare no competing financial interest.

## ACKNOWLEDGMENTS

We thank Emily Bernhardt and members of her lab for leading the CEINT mesocosm study as well as providing intellectual feedback. This material is based upon work supported by the National Science Foundation (NSF) and the Environmental Protection Agency (EPA) under NSF Cooperative Agreement EF-0830093, Center for the Environmental Implications of NanoTechnology (CEINT). This research was additionally supported by a NSF Graduate Research fellowship to C.S.W. and a fellowship from the China Scholarship Council to J.-F.P. Any opinions, findings, conclusions, or recommendations expressed in this material are those of the author(s) and do not necessarily reflect the views of the NSF or the EPA. This work has not been subjected to EPA review, and no official endorsement should be inferred.

## REFERENCES


(1) Hendren, C. O.; Mesnard, X.; Dröge, J.; Wiesner, M. R. Estimating production data for five engineered nanomaterials as a basis for exposure assessment. *Environ. Sci. Technol.* **2011**, *45*, 2562−2569.

(2) Blaser, S. A.; Scheringer, M.; MacLeod, M.; Hungerbühler, K. Estimation of cumulative aquatic exposure and risk due to silver: contribution of nano-functionalized plastics and textiles. *Sci. Total Environ.* **2008**, *390* (2−3), 396−409.

(3) Benn, T. M.; Westerhoff, P. Nanoparticle silver released into water from commercially available sock fabrics. *Environ. Sci. Technol.* **2008**, *42* (11), 4133−4139.

(4) Kaegi, R.; Voegelin, A.; Sinnet, B.; Zuleeg, S.; Hagendorfer, H.; Burkhardt, M.; Siegrist, H. Behavior of metallic silver nanoparticles in a pilot wastewater treatment plant. *Environ. Sci. Technol.* **2011**, *45* (9), 3902−3908.

(5) Yin, L.; Colman, B. P.; McGill, B. M.; Wright, J. P.; Bernhardt, E. S. Effects of silver nanoparticle exposure on germination and early growth of eleven wetland plants. *PLoS One* **2012**, *7* (10), e47674.

(6) Hossain, Z.; Mustafa, G.; Sakata, K.; Komatsu, S. Insights into the proteomic response of soybean towards $Al_2O_3$, ZnO, and Ag nanoparticles stress. *J. Hazard. Mater.* **2016**, *304*, 291−305.

(7) Navarro, E.; Piccapietra, F.; Wagner, B.; Marconi, F.; Kaegi, R.; Odzak, N.; Sigg, L.; Behra, R. Toxicity of Silver Nanoparticles to *Chlamydomonas reinhardtii*. *Environ. Sci. Technol.* **2008**, *42* (23), 8959−8964.

(8) Dash, A.; Singh, A. P.; Chaudhary, B. R.; Singh, S. K.; Dash, D. Effect of silver nanoparticles on growth of eukaryotic green algae. *Nano-Micro Lett.* **2012**, *4* (3), 158−165.

(9) He, D.; Dorantes-Aranda, J. J.; Waite, T. D. Silver Nanoparticle-Algae Interactions: Oxidative Dissolution, Reactive Oxygen Species Generation and Synergistic Toxic Effects. *Environ. Sci. Technol.* **2012**, *46* (16), 8731−8738.

(10) Zhang, T.; Pan, J.-F.; Hunt, D. E.; Chen, M.; Wang, B. Organic matter modifies biochemical but not most behavioral responses of the clam *Ruditapes philippinarum* to nanosilver exposure. *Mar. Environ. Res.* **2018**, *133*, 105−113.

(11) Gwin, C. A.; Lefevre, E.; Alito, C. L.; Gunsch, C. K. Microbial community response to silver nanoparticles and Ag+ in nitrifying activated sludge revealed by ion semiconductor sequencing. *Sci. Total Environ.* **2018**, *616*, 1014−1021.

(12) Shin, Y.-J.; Kwak, J. I.; An, Y.-J. Evidence for the inhibitory effects of silver nanoparticles on the activities of soil exoenzymes. *Chemosphere* **2012**, *88* (4), 524−529.

(13) Yang, Y.; Quensen, J.; Mathieu, J.; Wang, Q.; Wang, J.; Li, M.; Tiedje, J. M.; Alvarez, P. J. Pyrosequencing reveals higher impact of silver nanoparticles than $Ag^+$ on the microbial community structure of activated sludge. *Water Res.* **2014**, *48*, 317−325.

(14) Cao, C.; Huang, J.; Yan, C.; Liu, J.; Hu, Q.; Guan, W. Shifts of system performance and microbial community structure in a constructed wetland after exposing silver nanoparticles. *Chemosphere* **2018**, *199*, 661−669.

(15) Liang, Z.; Das, A.; Hu, Z. Bacterial response to a shock load of nanosilver in an activated sludge treatment system. *Water Res.* **2010**, *44* (18), 5432−5438.

(16) Choi, O.; Hu, Z. Size dependent and reactive oxygen species related nanosilver toxicity to nitrifying bacteria. *Environ. Sci. Technol.* **2008**, *42* (12), 4583−4588.

(17) Morones, J. R.; Elechiguerra, J. L.; Camacho, A.; Holt, K.; Kouri, J. B.; Ramírez, J. T.; Yacaman, M. J. The bactericidal effect of silver nanoparticles. *Nanotechnology* **2005**, *16* (10), 2346−2353.

(18) Alito, C. L.; Gunsch, C. K. Assessing the effects of silver nanoparticles on biological nutrient removal in bench-scale activated sludge sequencing batch reactors. *Environ. Sci. Technol.* **2014**, *48* (2), 970−976.

(19) Doolette, C. L.; McLaughlin, M. J.; Kirby, J. K.; Batstone, D. J.; Harris, H. H.; Ge, H.; Cornelis, G. Transformation of PVP coated silver nanoparticles in a simulated wastewater treatment process and the effect on microbial communities. *Chem. Cent. J.* **2013**, *7* (1), 46.

(20) Bernhardt, E. S.; Colman, B. P.; Hochella, M. F.; Cardinale, B. J.; Nisbet, R. M.; Richardson, C. J.; Yin, L. An Ecological Perspective on Nanomaterial Impacts in the Environment. *J. Environ. Qual.* **2010**, *39* (6), 1954−1965.

(21) Colman, B. P.; Arnaout, C. L.; Anciaux, S.; Gunsch, C. K.; Hochella, M. F., Jr; Kim, B.; Lowry, G. V.; McGill, B. M.; Reinsch, B. C.; Richardson, C. J.; Unrine, J. M.; Wright, J. P.; Yin, L.; Bernhardt, E. S. Low Concentrations of Silver Nanoparticles in Biosolids Cause Adverse Ecosystem Responses under Realistic Field Scenario. *PLoS One* **2013**, *8* (2), e57189.

(22) Ferry, J. L.; Craig, P.; Hexel, C.; Sisco, P.; Frey, R.; Pennington, P. L.; Fulton, M. H.; Scott, I. G.; Decho, A. W.; Kashiwada, S. Transfer of gold nanoparticles from the water column to the estuarine food web. *Nat. Nanotechnol.* **2009**, *4* (7), 441−444.

(23) Cleveland, D.; Long, S. E.; Pennington, P. L.; Cooper, E.; Fulton, M. H.; Scott, G. I.; Brewer, T.; Davis, J.; Petersen, E. J.; Wood, L. Pilot estuarine mesocosm study on the environmental fate of silver nanomaterials leached from consumer products. *Sci. Total Environ.* **2012**, *421*, 267−272.

(24) Chae, S.-R.; Hunt, D. E.; Ikuma, K.; Yang, S.; Cho, J.; Gunsch, C. K.; Liu, J.; Wiesner, M. R. Aging of fullerene $C_{60}$ nanoparticle suspensions in the presence of microbes. *Water Res.* **2014**, *65*, 282−289.

(25) Reinsch, B.; Levard, C.; Li, Z.; Ma, R.; Wise, A.; Gregory, K.; Brown, G., Jr; Lowry, G. Sulfidation of silver nanoparticles decreases *Escherichia coli* growth inhibition. *Environ. Sci. Technol.* **2012**, *46* (13), 6992−7000.

(26) Grün, A.-L.; Emmerling, C. Long-term effects of environmentally relevant concentrations of silver nanoparticles on major soil bacterial phyla of a loamy soil. *Environ. Sci. Eur.* **2018**, *30* (1), 31.




DOI: 10.1021/acs.est.8b06654
*Environ. Sci. Technol.* 2019, 53, 3268−3276

(27) Keller, A. A.; Lazareva, A. Predicted releases of engineered nanomaterials: from global to regional to local. *Environ. Sci. Technol. Lett.* **2014**, *1* (1), 65−70.
(28) Lowry, G. V.; Espinasse, B. P.; Badireddy, A. R.; Richardson, C. J.; Reinsch, B. C.; Bryant, L. D.; Bone, A. J.; Deonarine, A.; Chae, S.; Therezien, M.; Colman, B. P.; Hsu-Kim, H.; Bernhardt, E. S.; Matson, C. W.; Wiesner, M. R. Long-term transformation and fate of manufactured Ag nanoparticles in a simulated large scale freshwater emergent wetland. *Environ. Sci. Technol.* **2012**, *46* (13), 7027−7036.
(29) Shade, A.; Peter, H.; Allison, S. D.; Baho, D. L.; Berga, M.; Bürgmann, H.; Huber, D. H.; Langenheder, S.; Lennon, J. T.; Martiny, J. B. Fundamentals of microbial community resistance and resilience. *Front. Microbiol.* **2012**, *3*, 417.
(30) Yuan, L.; Richardson, C. J.; Ho, M.; Willis, C. W.; Colman, B. P.; Wiesner, M. R. Stress Responses of Aquatic Plants to Silver Nanoparticles. *Environ. Sci. Technol.* **2018**, *52* (5), 2558−2565.
(31) Colman, B. P.; Espinasse, B.; Richardson, C. J.; Matson, C. W.; Lowry, G. V.; Hunt, D. E.; Wiesner, M. R.; Bernhardt, E. S. Emerging Contaminant or an Old Toxin in Disguise? Silver Nanoparticle Impacts on Ecosystems. *Environ. Sci. Technol.* **2014**, *48* (9), 5229−5236.
(32) Colman, B. P.; Baker, L. F.; King, R. S.; Matson, C. W.; Unrine, J. M.; Marinakos, S. M.; Gorka, D. E.; Bernhardt, E. S. Dosing, not the Dose: Comparing Chronic and Pulsed Silver Nanoparticle Exposures. *Environ. Sci. Technol.* **2018**, *52* (17), 10048−10056.
(33) Yin, L.; Cheng, Y.; Espinasse, B.; Colman, B. P.; Auffan, M.; Wiesner, M.; Rose, J.; Liu, J.; Bernhardt, E. S. More than the ions: the effects of silver nanoparticles on *Lolium multiflorum*. *Environ. Sci. Technol.* **2011**, *45* (6), 2360−2367.
(34) Djoković, V.; Krsmanović, R.; Božanić, D. K.; McPherson, M.; Van Tendeloo, G.; Nair, P. S.; Georges, M. K.; Radhakrishnan, T. Adsorption of sulfur onto a surface of silver nanoparticles stabilized with sago starch biopolymer. *Colloids Surf., B* **2009**, *73* (1), 30−35.
(35) Kozich, J. J.; Westcott, S. L.; Baxter, N. T.; Highlander, S. K.; Schloss, P. D. Development of a dual-index sequencing strategy and curation pipeline for analyzing amplicon sequence data on the MiSeq Illumina sequencing platform. *Appl. Environ. Microbiol.* **2013**, *79* (17), 5112−5120.
(36) Yung, C.-M.; Ward, C. S.; Davis, K. M.; Johnson, Z. I.; Hunt, D. E. Insensitivity of diverse and temporally variable particle-associated microbial communities to bulk seawater environmental parameters. *Appl. Environ. Microbiol.* **2016**, *82* (11), 3431−3437.
(37) Edgar, R. C. Search and clustering orders of magnitude faster than BLAST. *Bioinformatics* **2010**, *26* (19), 2460−2461.
(38) Edgar, R. C. UPARSE: highly accurate OTU sequences from microbial amplicon reads. *Nat. Methods* **2013**, *10* (10), 996−998.
(39) Edgar, R. C.; Haas, B. J.; Clemente, J. C.; Quince, C.; Knight, R. UCHIME improves sensitivity and speed of chimera detection. *Bioinformatics* **2011**, *27* (16), 2194−2200.
(40) Angly, F. E.; Dennis, P. G.; Skarshewski, A.; Vanwonterghem, I.; Hugenholtz, P.; Tyson, G. W. CopyRighter: a rapid tool for improving the accuracy of microbial community profiles through lineage-specific gene copy number correction. *Microbiome* **2014**, *2* (1), 11.
(41) Marie, D.; Partensky, F.; Jacquet, S.; Vaulot, D. Enumeration and cell cycle analysis of natural populations of marine picoplankton by flow cytometry using the nucleic acid stain SYBR Green I. *Appl. Environ. Microbiol.* **1997**, *63* (1), 186−193.
(42) Ward, C. S.; Yung, C.-M.; Davis, K. M.; Blinebry, S. K.; Williams, T. C.; Johnson, Z. I.; Hunt, D. E. Annual community patterns are driven by seasonal switching between closely related marine bacteria. *ISME J.* **2017**, *11* (6), 1412−1422.
(43) Hunt, D. E.; Lin, Y.; Church, M. J.; Karl, D. M.; Izzo, L. K.; Tringe, S.; Johnson, Z. I. Relationship between abundance and specific activity of bacterioplankton in open ocean surface waters. *Appl. Environ. Microbiol.* **2013**, *79* (1), 177−184.
(44) Polz, M. F.; Cavanaugh, C. M. Bias in template-to-product ratios in multitemplate PCR. *Appl. Environ. Microbiol.* **1998**, *64* (10), 3724−3730.
(45) Segata, N.; Izard, J.; Waldron, L.; Gevers, D.; Miropolsky, L.; Garrett, W. S.; Huttenhower, C. Metagenomic biomarker discovery and explanation. *Genome Biology* **2011**, *12* (6), R60.
(46) Love, M. I.; Huber, W.; Anders, S. Moderated estimation of fold change and dispersion for RNA-seq data with DESeq2. *Genome Biol.* **2014**, *15* (12), 1.
(47) Lamendella, R.; Strutt, S.; Borglin, S. E.; Chakraborty, R.; Tas, N.; Mason, O. U.; Hultman, J.; Prestat, E.; Hazen, T. C.; Jansson, J. Assessment of the Deepwater Horizon oil spill impact on Gulf coast microbial communities. *Front. Microbiol.* **2014**, *5*, 130.
(48) Allison, S. D.; Martiny, J. B. H. Resistance, resilience, and redundancy in microbial communities. *Proc. Natl. Acad. Sci. U. S. A.* **2008**, *105* (Suppl. 1), 11512.
(49) Eisler, R. *Eisler's encyclopedia of environmentally hazardous priority chemicals*; Elsevier: 2007.
(50) Panáček, A.; Kvítek, L.; Smékalová, M.; Večeřová, R.; Kolář, M.; Röderová, M.; Dyčka, F.; Šebela, M.; Prucek, R.; Tomanec, O. Bacterial resistance to silver nanoparticles and how to overcome it. *Nat. Nanotechnol.* **2018**, *13* (1), 65−71S.
(51) Hunt, D. E.; Ward, C. S. A network-based approach to disturbance transmission through microbial interactions. *Front. Microbiol.* **2015**, *6*, 1182.
(52) Liu, J.; Hurt, R. H. Ion release kinetics and particle persistence in aqueous nano-silver colloids. *Environ. Sci. Technol.* **2010**, *44* (6), 2169−2175.
(53) Brown, J. H.; Gillooly, J. F.; Allen, A. P.; Savage, V. M.; West, G. B. Toward a metabolic theory of ecology. *Ecology* **2004**, *85* (7), 1771−1789.
(54) Silver, S. Bacterial silver resistance: molecular biology and uses and misuses of silver compounds. *FEMS Microbiology Reviews* **2003**, *27* (2−3), 341−353.
(55) Yung, C.-M.; Vereen, M. K.; Herbert, A.; Davis, K. M.; Yang, J.; Kantorowska, A.; Ward, C. S.; Wernegreen, J. J.; Johnson, Z. I.; Hunt, D. E. Thermally adaptive tradeoffs in closely-related marine bacterial strains. *Environ. Microbiol.* **2015**, *17* (7), 2421−2429.
(56) Shade, A.; Read, J. S.; Welkie, D. G.; Kratz, T. K.; Wu, C. H.; McMahon, K. D. Resistance, resilience and recovery: aquatic bacterial dynamics after water column disturbance. *Environ. Microbiol.* **2011**, *13* (10), 2752−2767.


DOI: 10.1021/acs.est.8b06654
*Environ. Sci. Technol.* 2019, 53, 3268−3276